LETTER OPEN

Chemogenetic activation of G_{12} signaling enhances adipose tissue browning

Signal Transduction and Targeted Therapy (2023)8:307 ; https://doi.org/10.1038/s41392-023-01524-2

Dear Editor,

Beige adipocytes, which increase energy expenditure by dissipating energy as heat, have gained attention as a therapeutic target for combating obesity.[1] Adipocytes express many types of G-protein-coupled receptors (GPCRs), each of which has a unique preference for the G_s, G_i, G_q, and G_{12} subfamilies. While the function of G_s-coupled β-adrenergic receptors in beige adipocyte induction is well established,[2] little is known about the function of G_{12}-coupled GPCRs beyond its suppressive roles in white adipocyte maturation.[3] In this study, we generated transgenic mice conditionally expressing a G_{12}-coupled designer GPCR using a Cre-loxP system and investigated the potential effects of G_{12} signaling on adipocyte biology.

We first sought to improve the G_{12}-coupling selectivity of the previously established G_{12}-coupled Designed Receptor Exclusively Activated by Designer Drugs (DREADD; M3D-GPR183/ICL3), which showed a leaky coupling to other G-protein subtypes such as G_o.[4] Using PRECOG,[5] a GPCR-coupling prediction algorithm, we designed six single-point mutants and assessed G-protein-coupling activity upon stimulation with the designer ligand, clozapine N-oxide (CNO) (Supplementary Fig. 1a). The $F^{1.57}V$ mutant (superscript denotes Ballesteros-Weinstein numbering) reduced off-target G_o coupling while maintaining G_{12} coupling and a surface expression level (Fig. 1a, Supplementary Fig. 1b). G-protein-coupling profiling of the $F^{1.57}V$ construct revealed preferential activation of G_{12} among the four G-protein subfamilies (Fig. 1b). We chose the $F^{1.57}V$ mutant of the M3D-GPR183/ICL3 construct (hereafter referred to as $G_{12}D$) for the following transgenic mouse study.

We generated mice expressing HA epitope-tagged $G_{12}D$ in adipocytes (adipo-$G_{12}D$ mice) by crossing the *Rosa26-LSL-G12D-IRES-GFP* mice (Supplementary Fig. 2a) with the *Adipoq-Cre* mice. Western blot analysis confirmed its selective expression in adipose tissue (Supplementary Fig. 2b). In the basal state (without CNO administration), body weights and adipose tissue weights were not significantly different between the adipo-$G_{12}D$ mice and their control littermates (the *Rosa26-LSL-G12D-IRES-GFP* mice) (Supplementary Fig. 2c–e).

We next tested the effects of chemogenetic G_{12} activation on white-adipose tissue (WAT) browning and glucose homeostasis. Both control and adipo-$G_{12}D$ mice were treated with daily intraperitoneal (i.p.) injections of CNO (1 mg/kg) for 5 days prior to tissue collection. RT-PCR analysis showed that the expressions of thermogenic and adipogenic genes in inguinal WAT (iWAT) (Fig. 1c, d) as well as thermogenic genes in brown-adipose tissue (BAT) (Fig. 1e) were not significantly different between the two genotypes. Consistent with these observations, hematoxylin-eosin (H&E) staining showed no obvious morphological changes in both iWAT and BAT (Fig. 1f, Supplementary Fig. 3a). Furthermore, glucose tolerance was unchanged between the two genotypes in both regular chow- and high-fat diet (HFD)-fed conditions (Supplementary Fig. 4a, b). Therefore, activation of G_{12} signaling alone does not affect WAT browning, BAT activation, or whole-body glucose homeostasis.

We then investigated the synergistic effects of G_{12} activation with G_s activation through β3AR stimulation. Chronic administration of the β3AR-selective agonist CL316,243 is a widely used method to induce WAT browning and BAT activation in mice. Both groups of the mice were administered with CL316,243 together with CNO (both 1 mg/kg i.p.) daily for 5 days and evaluated for WAT browning. qRT-PCR analysis revealed a significant upregulation of key thermogenic genes (*Ucp1*, *Cidea*, and *Elovl3*), but not adipogenic genes, in iWAT of the adipo-$G_{12}D$ mice (Fig. 1g, h). In the absence of CNO, the induction of the thermogenic genes was comparable between the genotypes (Supplementary Fig. 3f). Western blotting validated increased UCP1 protein levels in the adipo-$G_{12}D$ mice (Fig. 1i, j). H&E staining demonstrated the increased numbers of multilocular cells, typical morphology of beige adipocytes in the adipo-$G_{12}D$ mice (Fig. 1k, Supplementary Fig. 3d, e). In contrast to the effects observed in iWAT, BAT showed minimal synergistic effects of CNO and CL316,243 on thermogenic gene expression and histology (Fig. 1l, Supplementary Fig. 3b, c). To further analyze the pathways affected by $G_{12}D$ activation, we performed RNA-seq transcriptome analysis using iWAT RNA samples. Gene set enrichment analysis (GSEA) revealed that genes upregulated in the adipo-$G_{12}D$ mice were involved in oxidative phosphorylation, adipogenesis, and fatty acid metabolism pathways (Fig. 1m, Supplementary Fig. 5), which play key roles in the development of beige adipocytes. The emergence of the adipogenesis characteristics in the analysis is likely attributable to upregulation of genes involved in oxidative phosphorylation and fatty acid metabolism, because these genes also fall under the "adipogenesis" category in the GSEA. Downregulated gene sets were associated with the inflammatory response, such as interferon-α response and TNF-α signaling via NF-κB (Fig. 1m, Supplementary Fig. 5), which is involved in adipocyte dysfunction, including insulin resistance.

To explore the physiological significance of $G_{12}D$-enhanced WAT browning, we evaluated whole-body energy expenditure and adaptive thermogenesis. After simultaneous daily injections of CNO and CL316,243 (both 1 mg/kg i.p.) for 5 days at room temperature, the mice were placed in a metabolic chamber and oxygen consumption was monitored before and after the additional CNO and CL316,243 administration. An acute increase in oxygen consumption was observed in both groups of the mice following the drug administration, a phenomenon attributable to β3AR stimulation (Fig. 1n). In the adipo-$G_{12}D$ mice, the elevated oxygen consumption persisted over time, contrasting with the gradual decrease observed in the control mice (Fig. 1n, o). Under this condition, the blood glucose level was higher in the adipo-$G_{12}D$ mice while the free-fatty acid level was lower and the glycerol level was unchanged (Supplementary Fig. 6a–d), suggesting that β3AR-induced lipolysis remains unchanged, but fatty-acid

Received: 25 February 2023 Revised: 13 May 2023 Accepted: 28 May 2023
Published online: 21 August 2023

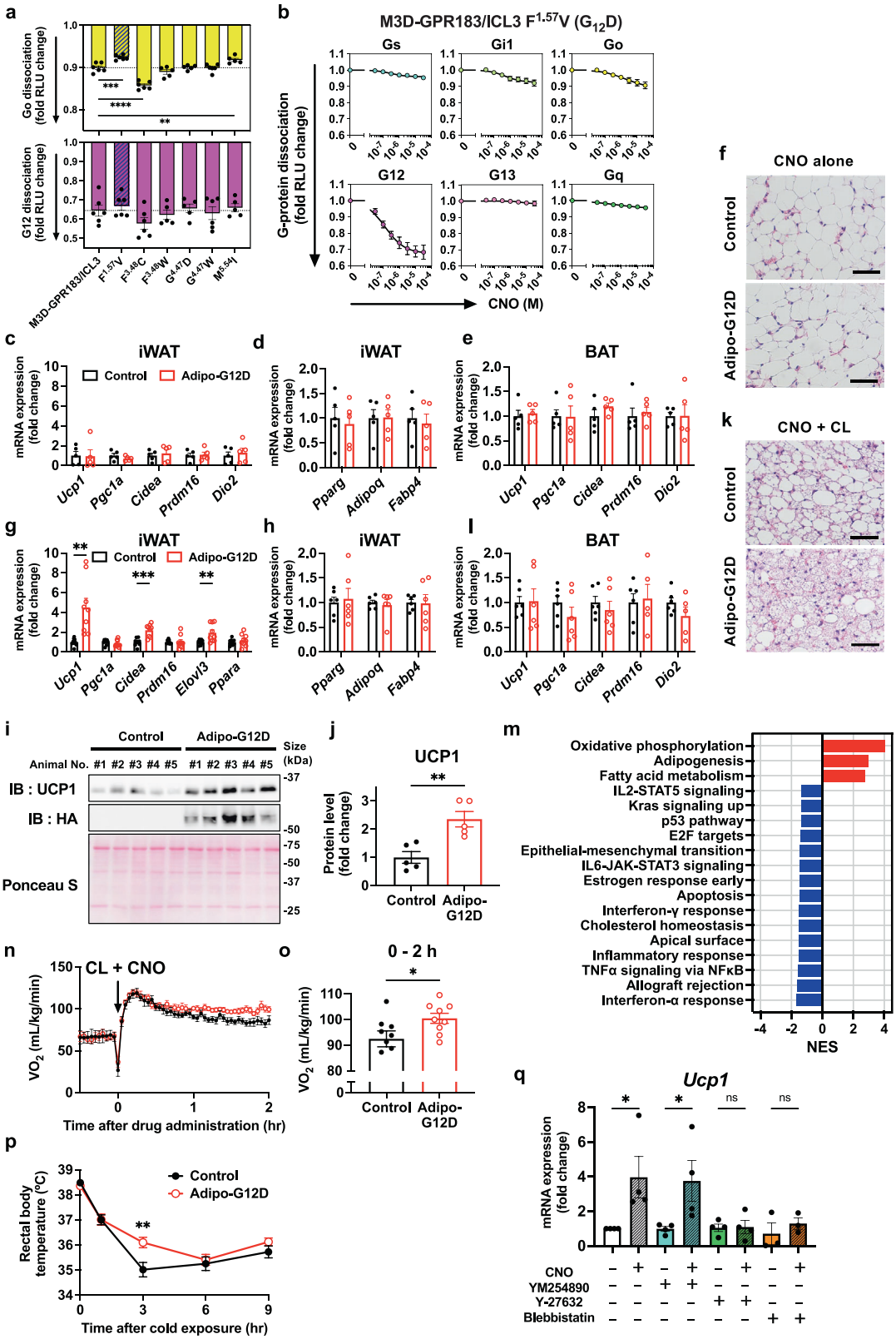

uptake is enhanced in the adipo-$G_{12}D$ mice. To examine adaptive thermogenesis, after the 5-day drug administration, the mice were placed in a 4 °C cold chamber and and their rectal body temperature was measured. While the control mice showed a rapid decrease in body temperature (peak at 3 h), the decrease rate in the adipo-$G_{12}D$ mice was slower (peak at 6 h) (Fig. 1p). Together, these results demonstrate functional significance of $G_{12}D$-induced beige adipocytes.

To investigate whether $G_{12}D$-induced enhancement of WAT browning is controlled in a cell-autonomous manner and to

Fig. 1 Synergistic induction of beige adipogenesis through the G_{12}-coupled designer GPCR and the G_s-coupled β3AR. **a** Functional screening of M3D-GPR183/ICL3-derived constructs for G_{12} selectivity. G_{12} and G_o activation was measured by the NanoBiT-G-protein dissociation assay with 10 μM CNO. Note that G-protein activation causes decrease in luminescence counts. Bars and error bars represent the mean and SEM, respectively, of 5-6 independent experiments (dots) with each performed in duplicate. The $F^{1.57}V$ mutant of the M3D-GPR183/ICL3 construct (oblique bars) is referred to as G_{12}-DREADD or G_{12}D. **b** Concentration-response curves for G-protein activation by the $F^{1.57}V$ M3D-GPR183/ICL3 construct. The G-protein-coupling profile was examined by the NanoBiT-G-protein dissociation assay using representative members of the four G-protein subfamilies. Symbols and error bars represent the mean and SEM, respectively, of 3–9 independent experiments with each performed in duplicate. **c**, **d** Expression of thermogenic (**c**) and adipogenic (**d**) genes in iWAT following CNO single-drug administration (1 mg/kg, i.p., daily) for 5 days ($n = 5$ per group). **e** Expression of thermogenic genes in BAT following CNO administration (1 mg/kg, i.p., daily) for 5 days ($n = 5$ per group). **f** Representative H&E staining of iWAT following CNO single-drug administration (1 mg/kg, i.p., daily) for 5 days (scale bar: 50 μm). **g**, **h** Expression of thermogenic (**g**) and adipogenic (**h**) genes in iWAT following CL316,243 and CNO dual-drug administration (1 mg/kg each, i.p., daily) for 5 days ($n = 9$ for (**g**) and 6 for (**h**) per group). **i**, **j** Ucp1 protein levels detected by immunoblotting in iWAT of the control and the adipo-G_{12}D mice treated dually with CL316,243 and CNO (1 mg/kg each, i.p., daily) for 5 days ($n = 5$ per group). **k** Representative H&E staining of iWAT following CL316,243 and CNO dual-drug administration (scale bar: 50 μm). **l** Expression of thermogenic genes in BAT following 1 mg/kg CL316,243 and 1 mg/kg CNO dual-drug administration for 5 days ($n = 5$ or 6 per group). **m** Significantly enriched gene sets (FDR < 0.05) in GSEA. Red: positive NES, blue: negative NES. **n**, **o** Whole-body energy expenditure. The mice that were pretreated dually with CL316,243 and CNO (1 mg/kg each, i.p., daily) for 5 days were placed in the metabolic chamber and oxygen consumption rate (VO_2) was monitored before and after the dual-drug administration (CL316,243 and CNO, 1 mg/kg each, i.p.; $n = 9$). Average VO_2 during post 2-h drug administration (**o**). **p** Rectal body temperature of the mice treated dually with CL316,243 and CNO (1 mg/kg each, i.p., daily) for 5 days upon acute exposure to 4 °C for the indicated time ($n = 12$ per group. **q** *Ucp1* expression in primary SVF cells stimulated with 10 μM CNO, with or without pretreatment of 10 μM YM-254890, 10 μM Y-27632, or 50 μM blebbistatin ($n = 3$ or 4 per group). In all figure panels, bars or symbols, and error bars represent mean and SEM, respectively. Statistical significance was determined by one-way ANOVA followed by the Dunnett's post-hoc test (**a**), the two-tailed Student's *t*-test (**c**–**e**, **g**, **h**, **j**, **l**), the two-way ANOVA followed by the Sidak's post-hoc test (**p**) or the one-way ANOVA followed by the Sidak's post-hoc test (**q**). $^*P < 0.05$, $^{**}P < 0.01$, $^{***}P < 0.001$, and $^{****}P < 0.0001$

understand the downstream mechanism, we performed a primary culture experiment. Stromal vascular fraction (SVF) was isolated from the adipo-G_{12}D mice and differentiated into beige adipocytes in vitro. After differentiation, beige adipocytes were stimulated with CNO in the presence or absence of a series of signaling inhibitors (a Rho kinase (ROCK) inhibitor Y-27632, a G_q inhibitor YM-254890, or a myosin II inhibitor blebbistatin). Stimulation by CNO enhanced *Ucp1* expression (Fig. 1q), indicating that G_{12}D-mediated *Ucp1* expression was at least partially cell-autonomous and that constitutive G_s signaling was induced in the culture condition. Furthermore, the enhancement of *Ucp1* expression was completely inhibited by pretreatment with Y-27632 and blebbistatin, but not by YM-254890 (Fig. 1q). This result demonstrates that G_{12}D-mediated *Ucp1* expression is dependent on ROCK and myosin II, canonical downstream effectors of G_{12}, and is not mediated by potential coupling of G_{12}D to G_q.

Since activation of G_{12} signaling by the DREADD system promoted WAT browning, we searched for G_{12}-coupled GPCRs that are endogenously expressed in adipocytes. Using previously published RNA-seq data of isolated mouse iWAT adipocytes, we identified 16 types of G_{12}-coupled GPCRs that are expressed in adipocytes (Supplementary Fig. 7).

In conclusion, we used our newly generated the adipo-G_{12}D mice to elucidate the effect of chemogenetic activation of G_{12} signaling in adipocytes. The G_{12} signaling was found to synergistically enhance the beige adipogenesis triggered by the G_s-coupled β3AR, thus potentiating the thermogenic effect in vivo. Although we hypothesize that the underlying mechanism is attributed to the synergistic effect downstream of G_s and G_{12} signaling, it is also conceivable that G_{12} signaling boosts the availability of cell-surface β3AR. Moreover, a study using the adpo-G_{12}D mice in the G_{12} (*Gna12*)-deficient background will serve as an important validation, which we plan to investigate in the future. Nevertheless, our finding highlights a previously unrecognized role for G_{12} signaling as a regulatory pathway of beige adipocyte induction. As G_{12} signaling remains uncharacterized in many other tissues, the use of the Cre-driven G_{12}D mice will expedite understanding of G_{12} signaling in physiology and pharmacology as well as drug development for G_{12}-coupled GPCRs.

DATA AVAILABILITY

All data generated in this study are included in the Source Data file. The RNA-seq data are viewable under the DDBJ accession number PRJDB14356.

ACKNOWLEDGEMENTS

We thank members of the Inoue laboratory for helpful discussion and manuscript editing; Francois Marie Ngako Kadji, Kayo Sato, Shigeko Nakano, and Ayumi Inoue (Tohoku University) for their assistance with plasmid preparation, the NanoBiT-GPCR assay and the flow cytometry analysis; Natsumi Hirai and Kouki Kawakami (Tohoku University) for their assistance of animal and cell-based experiments, respectively; Keita Iio and Keita Kajitani (University of Tsukuba) for their assistance of CNO synthesis; Jumpei Omi (The University of Tokyo) and Jurgen Wess (National Institute of Health) for helpful discussion; Atsushi Matsuzawa and Yoshihisa Tomioka (Tohoku University) for a support of the qPCR analysis. This work is supported by JP20J20669 (Y.O.), JP21H04791 (A.I.), JP21H05113 (A.I.), JPJSBP120213501 (A.I.) JPJSBP120218801 (A.I.), and JP21H05115 (T.S.) from The Japan Society for the Promotion of Science (JSPS); JPMJPR1331 (A.I.), JPMJFR215T (A.I.), JPMJMS2023 (A.I.) from the Japan Science and Technology Agency (JST); JP19gm5910013 (A.I.), JP19gm0010004 (A.I. and J.A.), JP20am0101095 (A.I.), JP22ama121038 (A.I.) and JP22zf0127007 (A.I.) from the Japan Agency for Medical Research and Development (AMED); Takeda Science Foundation (A.I.); The Uehara Memorial Foundation (A.I.); Tokyo Biochemical Research Foundation (A.I.); and Daiichi Sankyo Foundation of Life Science (A.I.). F.R. was supported by the Italian Ministry of University and Research through the Department of excellence "Faculty of Sciences" of Scuola Normale Superiore. The research leading to these results also received funding from the Italian Association for Cancer Research (AIRC) under My First AIRC Grant (MFAG) 2020—ID. 24317 project—P.I. Raimondi Francesco. G.S. and R.B.R. were funded by BMBF-funded de.NBI HD-HuB network, number #031A537C.

AUTHOR CONTRIBUTIONS

Conceptualization, Y.O. and A.I.; Investigation, Y.O. (animal experiments and SVF experiment), R.I. (SVF experiment and VO_2 experiment), K.A. (HFD experiment, VO_2 experiment and blood FFA experiment), G.S., R.B.R., F.R., A.I. (G_{12}D generation and evaluation), and T.S. (CNO synthesis); Writing, Y.O. and A.I. with feedback from all of the coauthors; Funding Acquisition, Y.O., F.R., JA, A.I.; Supervision, J.S., J.A., and A.I. All authors have read and approved the article.

ADDITIONAL INFORMATION

Supplementary information The online version contains supplementary material available at https://doi.org/10.1038/s41392-023-01524-2.

Competing interests: The authors declare no competing interests.

Ethics declarations: Mice were maintained according to the Guidelines for Animal Experimentation of Tohoku University, and the protocol was approved by the Institutional Animal Care and Use Committee at Tohoku University under the permission number of 2022PhA-001.

Yuki Ono[1], Ryo Ito[2], Kaito Arai[1], Gurdeep Singh[3,4], Tsuyoshi Saitoh[5,6], Robert B. Russell[3,4], Francesco Raimondi[7], Junken Aoki[8], Juro Sakai[2,9] and Asuka Inoue[1]✉
[1]*Molecular and Cellular Biochemistry, Graduate School of Pharmaceutical Sciences, Tohoku University, Sendai, Miyagi 980-8578, Japan;* [2]*Division of Molecular Physiology and Metabolism, Graduate School of Medicine, Tohoku University, Sendai, Miyagi 980-8574, Japan;* [3]*Bioquant, Heidelberg University, Im Neuenheimer Feld 267, 69120 Heidelberg, Germany;* [4]*Biochemie Zentrum Heidelberg (BZH), Heidelberg University, Im Neuenheimer Feld 328, 69120 Heidelberg, Germany;* [5]*International Institute for Integrative Sleep Medicine (WPI-IIIS), University of Tsukuba, 1-1-1 Tennodai, Tsukuba, Ibaraki 305-8575, Japan;* [6]*Graduate School of Comprehensive Human Sciences, University of Tsukuba, 1-1-1 Tennodai, Tsukuba, Ibaraki 305-8575, Japan;* [7]*Laboratorio di Biologia Bio@SNS, Scuola Normale Superiore, Piazza dei Cavalieri 7, Pisa 56126, Italy;* [8]*Department of Health Chemistry, Graduate School of Pharmaceutical Sciences, The University of Tokyo, Bunkyo-ku, Tokyo 113-0033, Japan and* [9]*Division of Metabolic Medicine, Research Center for Advanced Science and Technology, The University of Tokyo, Meguro-ku, Tokyo 153-8904, Japan*
These authors contributed equally: Ryo Ito, Kaito Arai
Correspondence: Asuka Inoue (iaska@tohoku.ac.jp)

REFERENCES

1. Harms, M. & Seale, P. Brown and beige fat: development, function and therapeutic potential. *Nat. Med.* **19**, 1252–1263 (2013).
2. Wu, J. et al. Beige adipocytes are a distinct type of thermogenic fat cell in mouse and human. *Cell* **150**, 366–376 (2012).
3. Yanagida, K. et al. The Gα12/13-coupled receptor LPA4 limits proper adipose tissue expansion and remodeling in diet-induced obesity. *JCI Insight* **3**, e97293 (2018).
4. Inoue, A. et al. Illuminating G-protein-coupling selectivity of GPCRs. *Cell* **177**, 1933–1947.e25 (2019).
5. Singh, G., Inoue, A., Gutkind, J. S., Russell, R. B. & Raimondi, F. PRECOG: PREdicting COupling probabilities of G-protein coupled receptors. *Nucleic Acids Res.* **47**, 395–401 (2019).